

Nonlinear cracking behavior of 2083 and 2083 ESR stainless steel used in core of injection mold

Mehmet Yüksel, Tarık Sivri, Ahmet Akkaya, Fatma Betül Ulusoy*

Petka Mold, Adana, Turkey

ABSTRACT

In this study, it is aimed to investigate nonlinear surface crack of 2083 stainless steel used in core of injection mold. Strength properties and microstructure of the material directly affect the final product properties and quality. Stress in the structure of steel occurs resulting from shaping and cooling during solidification. It is possible for the same stresses to occur in the structure of the steel that is subjected to machining to produce any mold or mold component from a steel whose production operations have been completed. These stresses that may cause dimensional changes during should be removed by annealing at a suitable temperature according to the type of steel used. This paper focused on the non-linear surface cracks which have been observed on the 2083 stainless steel used in core of injection mold. Also 2083 ESR (Electroslag Refining) stainless steel has been used for production injection mold in this study. It has not been observed any surface cracks. The same heat treatment with different temperature and time has been performed on the 2083 and 2083 ESR stainless steel. The metallographic analysis, chemical composition and hardness test have been performed for comparative analysis. It has been found that the 2083 stainless steel hardness value lower than 2083 ESR stainless steel at the same heat treatment process. It can be concluded that 2083 stainless steel has a coarse grain. It means that the heterogeneous microstructure negatively affects mechanical properties.

Keywords: Surface cracks, 2083 stainless steel, 2083 ESR stainless steel, metallographic analysis, injection mold

Copyright © 2024 by author(s), DergiPark and JOEBS. This work is licensed under the Creative Commons Attribution International License (CC BY 4.0).

[CC BY 4.0 Deed](#) | [Attribution 4.0 International](#) | [Creative Commons](#)

1. INTRODUCTION

Recently, PolyEthylene Terephthalate (PET) is widely used for production of bottle/container due to its excellent mechanical and barrier properties [1]. PET bottle is firmly established in the global packaging market with dynamic annual earnings. The versatility of PET in terms of size, shape and functionality is one of the factors that make it stand out in the market. The plastic bottle market is growing with increasing demand for polyethylene terephthalate (PET) plastic bottles due to their recyclability. In addition, the increasing production of polyethylene terephthalate (PET) plastic bottles due to their durability, reliability and environmental friendliness increases their cost-effectiveness. Thus, it also enables to increase the growth industry. In other words, the increasing demand for reusable plastic bottles due to increasing environmental awareness gives further impetus to market growth. The global polyethylene terephthalate PET bottle market reached US\$ 565.93 Billion in 2020 driven by increasing demand for polyethylene terephthalate (PET) plastic bottles. It has been expected to reach USD 781.90 Billion by 2028, displaying a CAGR of 3.87 % from 2021-2028. The PET bottles production process is defined by two process

stages which is injection and blowing process. The machine that can be called conventional production method is widely used to produce injection and blowing molding process. Machining is one of the most common manufacturing methods where the final shape is given by traditionally removing shavings from the metal material surface with cutting tools. The injection form occurs by stretching and blowing at the same time during the process. This process is performed in a mold which has a desired shape, technical and physical properties. The process stability is directly affecting the final product quality, uniformity in form distribution because of thermomechanical process [2]. The preform is obtained by injecting polyethylene terephthalate (PET) in the mold at a certain temperature. The temperature distribution along the length of the performance is one of the most important parameters in this stage. The temperature directly affects consistency of raw material and influences kinematics during preform forming process. The point between the blown preform and cooler mold walls reduce the blown preform temperature because of temperature difference. This temperature difference enables the solidification of plastic initiates [3]. The production phase in pet blow molding machines takes place in the feeding unit of the blow molding machines of the preforms produced in the injection machines. The preform heating process is one of the most important stages for the bottle to take the desired form in the mold. It is important to ensure that the same wall thickness is achieved in every part of the bottle [4]. The blowing phase is performed at high pressure and in a very short time. The first blowing of 4-6 bars is performed in the preform. Then this pressure reaches about 15-40 bars that is value completed the final shape of bottle. Nonuniform temperature distribution of preform, waste air pressure in mold directly affects final product quality. Also, the

* betül.uluso@petkamold.com

material selection which is used in injection and blowing mold production is one of the most crucial points for ensuring final product quality and mold life. The internal stress which can be raised from machining process can be caused by non-linear surface cracks on the material in progress of time. Much research has been studied about that the understanding of metal deformation and fracture, but these mechanisms cannot be explained exactly. Recently the studies of single crystals which have a simple structure have been examined for understanding these mechanisms [5]. Fatigue cracks are considered to arise from a variety of mechanisms in steels. These mechanisms can be categorized such as surface at machining marks, grain/phase boundaries defects or internal metallurgical defects [6]. It has been reported that the formation of cracks can occur only if there are stresses. Also, it has been reported that the level of the ductility of the steel is directly affected by the level of stresses which are responsible for crack forming in the related material [7]. Steelmaking technology has a critical role in ensuring high-quality steel melts because of formation of the reoxidation of melt occurs. Thus, this cause to increase inclusion content in the raw material [8]. The electroslag refining process admitted process for the high-quality raw materials production [9]. Electroslag Refining process can be defined is one of the refining processes. This process provides a thin slag layer solidifies on the surface of the raw material. Also, this ensures a smooth surface quality [10]. ESR process ensures to obtain raw materials which have a minimum inclusion content, good chemical homogeneity, and homogeneous structure leading improvement in mechanical properties [11]. It is possible to obtain the highest mechanical properties such as ductility and toughness by using ESR process compared to conventional process [12].

2.1. MATERIAL AND METHOD

2.1.1. CORE

The injection blow molding machine has a hot and cold two different part contain entire injection unit and table which has a multi-impression mold assembly mounted on the rotary table [13]. The injection mold contains different components which have different dimensions, wall thickness, length. The core is one of the most important components of the injection mold structure. On the other words the core has been used for forming of PET preform during solidification of plastic initiate's process. Figure 1 shows the core design.

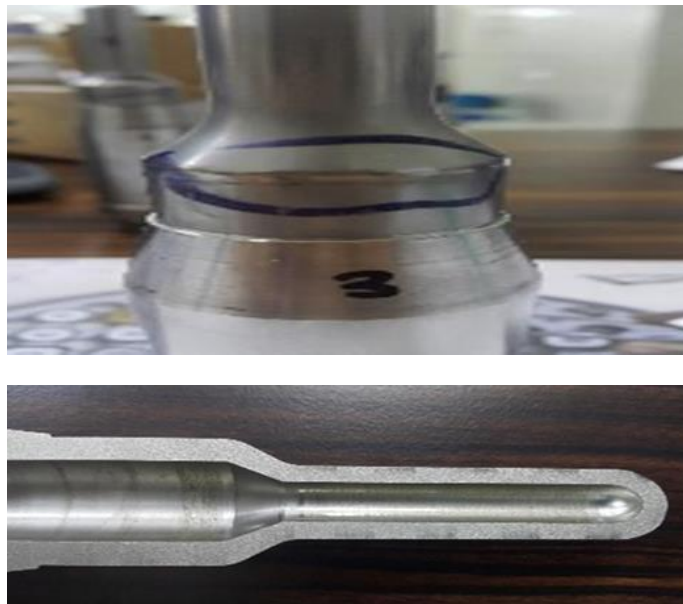


Figure 1. The core design 2083 and 2083 ESR stainless steel chemical composition analysis

2.1.2. 2083 and 2083 ESR STAINLESS STEEL CHEMICAL COMPOSITION ANALYSIS

Stainless steel has a wide range of applications for various purposes in many different industries due to their properties such as corrosion resistant, high tensile strength, easy formation [14]. Table 1 and Table 2 show the chemical composition of 2083 and 2083 ESR stainless steel has been used in this study. The chemical analysis has been performed using spectral analysis.

Table 1. Chemical composition of 2083

C	Mn	P	S	Si	Cr
0.358	0.227	0.0184	0.000	0.454	13.2
			5		
Fe	Mo	Ni	Cu	Pb	Al
85.1	0.762	0.156	0.060	0.0020	0.0166
			5		
Co	Ti	V	W	Sn	B
0.0204	0.0055	0.0466	0.022	0.0045	0.0002
			6		

Table 2. Chemical composition of 2083 ESR

C	Mn	P	S	Si	Cr
0.417	0.730	0.0181	0.0037	0.96	13.0
				2	
Fe	Mo	Ni	Cu	Pb	Al
84.4	0.0113	0.179	0.0405	0.0020	0.012
					2
Co	Ti	V	W	Sn	B
0.0232	0.0076	0.0728	0.0161	0.0056	0.000
					6

2083 stainless steel is equivalent to AISI 420 steel. Main

characteristics of DIN 2083 are listed such as a good atmospheric resistance, excellent machinability in annealed condition, good wear resistance.

3. EXPERIMENTAL

3.1. CORE PRODUCTION PROCESS

The core production process contains different machines such as roughing cut, perforation, heat treatment, finish. The heat treatment has been performed for stainless steel is given Table 3.

Table 3. Heat treatment process for 2083 and 2083 ESR stainless steel

Step	Process	Temperature and Time
Step-1	Pre-heating	650°C, 1-2 hours
Step-2	Second heating	800°C, 1-2 hours
Step-3	Hardening	1020-1040°C, 15-30 minutes
Step-4	Cooling	550°C, 2-3 minutes 30°C, 2-3 hours
Step-5	Tempering	300°C, 5-6 hours 150-200°C, 2-3 minutes 30°C, 2-3 hours
Step-6	Tempering	300°C, 5-6 hours 150°C, 2-3 minutes 30°C, 2-3 hours

The hardening stage with 1020-1040 °C and 15-30 minutes is defined austenite point temperature. The cooling process was performed using nitrogen gases. The hardness of the material should be checked after the first tempering process.

4. RESULTS AND DISCUSSION

4.1. NONLINEAR SURFACE CRACKS

Figure 2 shows that the core has a surface crack. The internal hole surface quality of core tends to corrosion formation. Also, this corrosion causes cracks on the core surface.



Figure 2. Core surface cracks

4.2. HARDNESS TEST

Table 4 and Table 5 show the numerical data of absorb energy, preexperimental and postexperimental. 150 Joule Hammer has been used during experiment. The hardness values which are obtained post-experimental arise from tensile and compression force. It has been found that the absorb energy exhibits a different distribution for each test sample of 2083. It can be concluded that the amount in internal structure of this material. Also, this impurity is dispersed heterogeneously in the raw material.

Table 4. Test results of 2083 stainless steel

Test No	Absorb Energy (Joule)	Hardness (preexperimental) (HRC)	Hardness (postexperimental) (HRC)
1	21	19.5-21.5	10.9
2	37.5	19.5-21.5	13.3
3	34.1	19.5-21.5	10.15
4	12.1	19.5-21.5	13.25

Table 5. Test results of 2083 ESR stainless steel

Test No	Absorb Energy (Joule)	Hardness (preexperimental) (HRC)	Hardness (postexperimental) (HRC)
1	13.4	24.5-27.5	13.35
2	14.8	24.5-27.5	13.1
3	14.6	24.5-27.5	13.7
4	11	24.5-27.5	13.45

It can be seen clearly that 2083 sample has a lower hardness value than 2083 ESR sample in Table 2. It can be concluded that 2083 sample has a coarse-grained than 2083 ESR sample.

4.1. METALLOGRAPHIC TEST

Spruers Transpol-2 sample preparation device was used. Also 60-120-240-400-500-800-1000-1200 Grit SiC emery and 1-3-6-9-

micron polishing broadcloth. The metallographic test was performed for different samples of the DIN 1.2083 stainless steel used in core of injection mold. Thus, it was aimed to investigate different unit areas on the same base metal using metallographic test. These samples were categorized with 4 different sample numbers. Figure 3 shows sample 1 metallographic test with different magnification factor (200X and 500X) for 2083.



a)



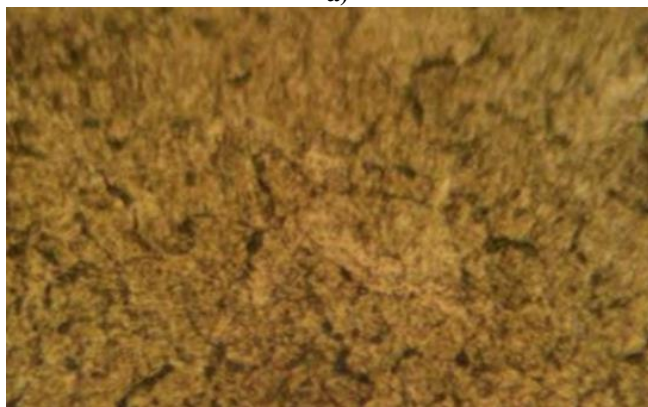
b)

Figure 3. Metallographic test of 2083 stainless steel with a) 200X b) 500X

It was observed that nonhomogeneous structure is based on martensitic-ferrite microstructure. Figure 4 shows sample 2 metallographic tests with different magnification factor (200X and 500X) for 2083 ESR stainless steel.



a)



b)

Figure 4. Metallographic test of 2083 ESR stainless steel with a) 200X b) 500X

It can be seen clearly that 2083 ESR has a martensite structure in Figure 4. The structure exhibits homogeneous characterization. Also, it was observed that the carbide precipitates in the structure. This precipitates can be related to the heat treatment process. Ni et al. has focused on the ESR process on the microstructure and mechanical properties of TiC particle reinforced 304 stainless steels. Also, they have observed that there is more uniform distribution in the microstructure [15]. Qui et al. have focused on the effect of ESR process on the inclusions. They have reported that ESR process remove the large inclusions and improve the distribution of inclusions [16]. Kim [17], Sawahata [18], Tanigawa [19], Li [20], Xia [21] and Sakasegawa [22] have been reported that ESR process has significant affect the inclusion, microstructure, and mechanical properties of the reduced activated ferritic/martensitic (RAFM) steels.

5. CONCLUSION

In this study, the comparative analysis has been aimed between 2083 and 2083 ESR stainless steel in terms of hardness value, structural characterization. Also, the effect of heat treatment on the structure characterization has been analyzed. It can be concluded that the gross amount of 2083 stainless steel is higher than 2083 ESR stainless steel. This gross and can be defined as an impureness can be cause to heterogeneous structure in the raw material which is used for core production process. It means that impureness directly affects the mechanical properties of the raw material. And this impurity of the

microstructure causes stress during the machining process of raw material. It can be concluded that the ESR process provides minimum inclusion in the micro-structure of the raw material. Thus, it has not been observed that any surface cracks on the injection mold which is produced from 2083 ESR stainless steel.

REFERENCES

[1] Daver F., Demirel B., 2012. Experimental study of perform reheat temperature in two-stage injection stretch blow molding. *Polymer Engineering and Science*, 53, 4, 868-873.

[2] Daver F., Demirel B., 2012. A simulation study of the effect of preform cooling time in injection stretch blow molding. *Journal of Materials Processing Technology*, 212, 11, 2400-2405.

[3] Lontos A., Gregoriou A., 2018. A numerical investigation of the effect of preform length for the fabrication of 1.5 Lt PET bottle through the injection stretch blow molding process. *MATEC Web of Conferences*, 188, 01021

[4] Venkateswaran G., Cameron M. R., Jabarin S. A., 1998. Effect of temperature profiles through preform thickness on the properties of re-heat blown PET containers. *Advances in Polymer Technology*, 17, 3, 237-249.

[5] Qiao L. J., Gao K. W., Volinsky A. A., Li X. Y., 2011. Discontinuous surface cracks during stress corrosion cracking of stainless-steel single crystal. *Corrosion Science*, 53, 3509-3514.

[6] Gaur V., Doquet V., Persent E., Mareau C., Roguet E., Kittel J. 2015. Surface versus internal fatigue crack initiation in steel: influence of mean stress. *Internal Journal of Fatigue*, 82, 437-448.

[7] Louhenkilpi S., 2014. Continuous casting of steel. *Treatise on Process Metallurgy*, 373-434.

[7] Arh B., Podgornik B., Burja J., 2016. Electroslag remelting: a process overview. 2016. *Material Technology*, 50(6), 971-979.

[8] Kharicha A., Schützenhöfer W., Ludwig A., Tanzer R., Wu M., 2008. On the importance of electric currents flowing directly into the mould during an ESR process. 2008. *Steel Research International*, 79 (8), 632-636.

[9] Dojcinovic M., 2011. Comparative cavitation erosion test on steels produced by ESR and AOD refining. *Materials Science-Poland*, 29 (3), 216-222.

[10] Maity S. K., Ballal N. B., Goldhahn G., Kawalla R., 2009. Development of ultrahigh strength low alloy steel through electroslag refining process. *ISIJ International*, 49, 902-910.

[11] Taya M., 1991. Strengthening mechanisms of metal matrix composites. *Materials Transactions*, 32 (1), 1-19.

[12] Ebnesajjad S., 2003. Other molding techniques. *Melt Processible Fluoroplastic*, 273-315.

[13] Gowthaman P. S., Muthukumaran P., Gowthaman J., Arun C. 2017. Review on mechanical characteristics of 304 stainless steel using SMAW welding. *MASK International Journal of Science*

and Technology Vol 2.

[14] Ni Z., Sun Y., Xue F., Zhou J., Bai J., 2011. Evaluation of electroslag remelting in TiC particle reinforced 304 stainless steel. 2011. *Material Science and Engineering A*, 528 (18), 5664-5669.

[15] Qui G., Zhan D., Li C., Yang Y., Jiang Z., Zhang H., 2019. Effects of electroslag remelting process and Y on the inclusions and mechanical properties of the CLAM steel. *Nuclear Engineering and Technology*.

[16] Kim D., Park K. 2015. Effect of electroslag remelting process on low cycle fatigue property of reduced activation ferritic/martensitic steels. *New and Renewable Energy*, 11(4), 62-70

[17] Sawahata A., Tanigawa H., Enomoto M. 2008. Effect of electroslag remelting on inclusion formation and impact property of reduced activation ferritic/martensitic steels. *Journal of the Japan Institute of Metals*, 72(3), 176-180.

[18] Tanigawa W., Sawahata A., Sokolov M. A., Enomoto M., Klueh R. L., Kohyama A. 2007. Effects of inclusions on fracture toughness of reduced activation ferritic/martensitic F82H-IEA steels. *Materials Transactions*, 48(3), 570-573.

[18] Li S., J., Huang Q., Li C., Huang B. 2007. Influence of nonmetal inclusions on mechanical properties of CLAM steel. *Materials Transactions*, 48, 570-573.

[19] Xia Z. X., Zhang C., Lan H., Yang Z. G., Wang P. H., Chen J. M., Xu Z. Y., Li X. W., Li S. 2010. Influence of smelting processes on precipitation behaviors and mechanical properties of flow activation ferrite steels. *Materials Science and Engineering: A*, 528(2), 657-662.

[20] Sakasegawa H., Tanigawa H., Kano S., Abe H. 2015. Material properties of the F82H in an electric arc furnace. *Fusion Engineering and Design*, (98-99), 2068-20

